Poisson model of multilayer broken clouds

S.M. Prigarin, T.B. Zhuravleva, and P.V. Volikova

Institute of Computational Mathematics and Mathematical Geophysics, Siberian Branch of the Russian Academy of Sciences, Novosibirsk
Institute of Atmospheric Optics, Siberian Branch of the Russian Academy of Sciences, Tomsk

Received June 11, 2002

A Poisson model of multilayer broken clouds with correlations between layers is proposed. We discuss the results of a numerical experiment, in which the radiative characteristics of two-layer clouds are calculated by the Monte Carlo method. It is shown that the correlation between cloud layers can substantially affect the mean radiative fluxes.

Introduction

The partial cloud cover can be present in the atmosphere simultaneously at several levels. The observations[1] show that the presence or absence of clouds within different cloud layers can correlate. For instance, the probability of simultaneous occurrence of *Cumulonimbus* and *Cirrus* clouds in the tropics is quite high; whereas the simultaneous presence of *Cumulus* and *Stratus* anticorrelate. Also, it is well known that one cloud type (such as *Altostratus* and *Altocumulus*) can simultaneously be present at different atmospheric levels, making up a multilayer (up to 4–6 layers) cloud system, with length of the gaps between clouds ranging from a few meters to a kilometer.

Despite the fact that the clouds at different levels are either correlated or anticorrelated, general circulation models (GCMs) of the atmosphere predict cloud fraction *independently* in each individual layer, without taking into account the vertical correlations between the components of the complex cloud systems. The hypothesis of random overlap, first formulated by Manabe and Strickler[2] and widely used now in radiation calculations, assumes that all cloud layers are independent. Its use leads to overestimation of total cloud fraction. To partially improve the results, Geleyn and Hollingsworth[3] suggested an approach referred to as the “mixed overlap.” Essentially, it uses the hypothesis of random overlap for clouds from different levels, and the hypothesis of maximum overlap for cloud layers at the same level. The results obtained by Tian and Curry[4] showed that this brings the experimental and calculated total cloud amounts into closer agreement. However, one should remember that the hypothesis of mixed overlap (or its modifications) can only be used for calculation of radiative characteristics averaged over the area comparable with that of GCM grid cell (usually, 300 to 1000 km^2 as large). For a more detailed study of the influence of vertical cloud structure on the radiative cloud effects, other approaches are required.

The existing methods of studying the radiative transfer in the presence of multilayer clouds at the level of mesoscale processes can be conventionally divided into two groups. On the one hand, those are the approaches proposed, for instance, by Liang and Wang[5] and by Stubenrauch et al.[6]; ultimately, they are based on solution of equation of radiative transfer in a horizontally homogeneous medium.

The methods of the other group calculate the mean fluxes of solar and thermal radiation using the mathematical models of stochastic cloud structure, actively developed at present (see, e.g., Refs. 7–12) and adaptable to treat multilayer clouds. Oreopoulos and Barker[13] have suggested a model of multilayer clouds, obtained using transects (along XOY plane) of horizontally inhomogeneous cloud layer, in which the distribution of optical depth is described by the gamma distribution. The model considered in Ref. 14 assumes the *statistical independence* of cloud fields, from different layers. The model used in Ref. 15 makes it possible to describe the radiation regime of *correlated* cloud fields; however, it uses, as input parameters (precisely which are “responsible” for the correlation of clouds at different layers), the characteristics that are difficult to determine experimentally.

In the present paper, the well-known Poisson model of broken clouds is generalized for few-level clouds. The model allows one to construct the realizations of statistically independent cloud layers and study the influence of correlations between clouds at different atmospheric levels on the radiative transfer in the cloudy atmosphere.

1. Poisson model of multilayer broken clouds

1.1. Single-layer model

We will now describe the structure and properties of a Poisson model of single-layer broken clouds developed in Refs. 7, 16–19. Within this model, the geometry of cloud field is described by the random indicator function of the cloud occurrence $\kappa(\mathbf{r})$, $\mathbf{r} = (x, y, z)$, defined in the layer $H_{\text{bot}} \le z \le H_{\text{top}}$. The values of indicator function do not depend on z; while in the plane XOY within the simulation domain $[0, R_x] \times [0, R_y]$, they are determined via random field $\xi(\boldsymbol{\rho}) = \kappa(\mathbf{r})$, $\boldsymbol{\rho} = (x, y)$, constructed as follows. We shall consider the Poisson point fluxes $\{x_i\}$ and $\{y_j\}$ along the OX and OY axes, with the intensities A_x and A_y, respectively. In each rectangle $[x_i, x_{i+1}] \times [y_j, y_{j+1}]$, the random field $\xi(\boldsymbol{\rho})$ assumes the value 1 (cloud is present) with the probability p and 0 (cloud is absent) with the probability $(1 - p)$. For each rectangle, the values of the indicator function are chosen independently.

Now remind the properties of a Poisson point flux with the intensity A:

– the distance Δ between the neighboring points of the flux is distributed according to the exponential law (with the parameter A) with the density

$$\varphi(\Delta) = A \exp(-A\Delta), \quad \Delta > 0,$$

distribution function

$$\Phi(x) = P\{0 \le \Delta \le x\} = 1 - \exp(-A\Delta),$$

mathematical expectation $M\Delta = 1/A$, and variance $D\Delta = 1/A^2$;

– the number $n(L)$ of the points of the flux on the set of length L satisfies the Poisson law with the parameter AL:

$$P\{n(L) = k\} = \exp(-AL)\,(AL)^k/k!, \quad k = 0, 1, 2, \ldots,$$

whose mathematical expectation and variance are

$$Mn(L) = Dn(L) = AL,$$

i.e., the intensity of the Poisson flux A is equal to the mean number of points on a unit interval.

Thus, the points of the Poisson flux on an interval can be simulated in two ways: either successively (such as in order of increasing magnitude) with the exponential distribution between the neighboring points, or by "seeding" the points uniformly on a segment, with the number of points simulated beforehand in accordance with the Poisson distribution.

For the first two moments of the $\xi(\boldsymbol{\rho})$ field, the following relations hold:

$$M\xi(\boldsymbol{\rho}) = p, \quad M\xi(\boldsymbol{\rho}_1)\,\xi(\boldsymbol{\rho}_2) =$$
$$= P\{\xi(\boldsymbol{\rho}_1) = 1, \xi(\boldsymbol{\rho}_2) = 1\} = pV(\boldsymbol{\rho}_1, \boldsymbol{\rho}_2), \quad (1)$$

where p is the unconditional probability and $V(\boldsymbol{\rho}_1, \boldsymbol{\rho}_2)$ is the conditional probability of the cloud occurrence (at a point $\boldsymbol{\rho}_1$ given that the point $\boldsymbol{\rho}_2$ is in the cloud):

$$V(\boldsymbol{\rho}_1, \boldsymbol{\rho}_2) = P\{\xi(\boldsymbol{\rho}_1) = 1/\xi(\boldsymbol{\rho}_2) = 1\} = p + (1 - p) \times$$
$$\times \exp\{-A_x|x_1 - x_2| - A_y|y_1 - y_2|\}. \quad (2)$$

Obviously, the cloud fraction N for this model is given by the equality $N = p$; while the conditional probability $V(\boldsymbol{\rho}_1, \boldsymbol{\rho}_2)$ is more convenient in the form

$$V(\boldsymbol{\rho}_1, \boldsymbol{\rho}_2) = p + (1 - p)\exp\{-A(\boldsymbol{\omega}) \times |\boldsymbol{\rho}_1 - \boldsymbol{\rho}_2|\}, \quad (2a)$$

where

$$\boldsymbol{\omega} = (a, b) = (\boldsymbol{\rho}_1 - \boldsymbol{\rho}_2)/|\boldsymbol{\rho}_1 - \boldsymbol{\rho}_2|,$$

$$A(\boldsymbol{\omega}) = A_x|a| + A_y|b|.$$

Thus, the random function $\xi(\boldsymbol{\rho})$ is statistically homogeneous and anisotropic, and has the mathematical expectation $M\xi(\boldsymbol{\rho}) = p$, variance $D\xi(\boldsymbol{\rho}) = p\,(1 - p)$, and exponential normalized correlation function

$$B(\boldsymbol{\rho}_1, \boldsymbol{\rho}_2) = \exp\{-A(\boldsymbol{\omega}) \times |\boldsymbol{\rho}_1 - \boldsymbol{\rho}_2|\}.$$

To adjust to experimental data, it was suggested in Ref. 20 to use the empirical fit

$$A_x = [1.65\,(N - 0.5)^2 + 1.04]/D_x,$$
$$A_y = [1.65\,(N - 0.5)^2 + 1.04]/D_y, \quad (3)$$

where D_x and D_y are the mean horizontal sizes of an individual cloud along OX and OY directions.

1.2. Multilayer clouds

Now describe the model of multilayer broken clouds. We assume that each of the M nonintersecting cloud layers occupies the region of the space

$$H_{\text{bot}}^{(m)} \le z \le H_{\text{top}}^{(m)}, \quad m = 1, 2, \ldots, M,$$

where $H_{\text{bot}}^{(m)}$ and $H_{\text{top}}^{(m)}$ are the heights of bottom and top of the mth cloud layer, and

$$H_{\text{top}}^{(m)} \le H_{\text{bot}}^{(m+1)}, \quad m = 1, 2, \ldots, M - 1.$$

A modification of the Poisson model, proposed here for multilayer broken clouds, is based on the following main principle:

on the same realization of the Poisson fluxes $\{x_i\}$ and $\{y_j\}$ (with intensities A_x and A_y along OX and OY axes) for each layer an indicator function (field) $\xi_m(\boldsymbol{\rho})$, $\boldsymbol{\rho} = (x, y)$, $m = 1, 2, \ldots, M$, is constructed;

the random vectors $[\xi_1(\boldsymbol{\rho}), \xi_2(\boldsymbol{\rho}), \ldots, \xi_M(\boldsymbol{\rho})]$ are simulated independently for each rectangle $[x_i, x_{i+1}] \times [y_j, y_{j+1}]$; the vector components themselves, i.e., the values $\xi_m(\boldsymbol{\rho})$ for different $m = 1, 2, \ldots, M$, can be dependent.

Consider now the following model parameters:

$$p_m = P\{\xi_m(\boldsymbol{\rho}) = 1\},$$

$$P_{nm} = P\{\xi_n(\boldsymbol{\rho}) = 1, \xi_m(\boldsymbol{\rho}) = 1\}, \quad (4)$$
$$Q_{nm} = P\{\xi_n(\boldsymbol{\rho}) = 1/\xi_m(\boldsymbol{\rho}) = 1\},$$
$$\bar{Q}_{nm} = P\{\xi_n(\boldsymbol{\rho}) = 1/\xi_m(\boldsymbol{\rho}) = 0\}.$$

For these parameters, simple relations hold:

$$P_{nm} = p_n Q_{mn} = p_m Q_{nm},$$

$$Q_{mn} \in [0, \min(p_m/p_n, 1)], \quad Q_{nm} \in [0, \min(p_n/p_m, 1)],$$

$$p_n = Q_{nm}\,p_m + \bar{Q}_{nm}\,(1 + p_m).$$

The latter equality is proved as follows:

$$p_n = P\{\xi_n(\boldsymbol{\rho}) = 1\} = P\{\xi_n(\boldsymbol{\rho}) = 1 / \xi_m(\boldsymbol{\rho}) = 1\}\, P\{\xi_m(\boldsymbol{\rho}) = 1\} + P\{\xi_n(\boldsymbol{\rho}) = 1 / \xi_m(\boldsymbol{\rho}) = 0\}\, P\{\xi_m(\boldsymbol{\rho}) = 0\} = Q_{nm}\, p_m + \bar{Q}_{nm}\,(1 - p_m).$$

The correlations between random fields ξ_n and ξ_m are expressed as

$$K_{nm}(\boldsymbol{\rho}_1, \boldsymbol{\rho}_2) = M[\xi_n(\boldsymbol{\rho}_1) - M\xi_n(\boldsymbol{\rho}_1)] \times [\xi_m(\boldsymbol{\rho}_2) - M\xi_m(\boldsymbol{\rho}_2)] = M\xi_n(\boldsymbol{\rho}_1)\, \xi_m(\boldsymbol{\rho}_2) - p_n\, p_m = (p_n\, Q_{mn} - p_n\, p_m) \exp\{- A(\boldsymbol{\omega}) \times |\boldsymbol{\rho}_1 - \boldsymbol{\rho}_2|\}. \quad (5)$$

Indeed,

$$P\{\xi_n(\boldsymbol{\rho}_1) = 1,\ \xi_m(\boldsymbol{\rho}_2) = 1\} = P\{\xi_n(\boldsymbol{\rho}_1) = 1\} \times P\{\xi_m(\boldsymbol{\rho}_2) = 1 / \xi_n(\boldsymbol{\rho}_1) = 1\} = p_n\, \{P\{\xi_m(\boldsymbol{\rho}_2) = 1 / \xi_m(\boldsymbol{\rho}_1) = 1\} \times P\{\xi_m(\boldsymbol{\rho}_1) = 1 / \xi_n(\boldsymbol{\rho}_1) = 1\} + P\{\xi_m(\boldsymbol{\rho}_2) = 1 / \xi_m(\boldsymbol{\rho}_1) = 0\} \times P\{\xi_m(\boldsymbol{\rho}_1) = 0 / \xi_n(\boldsymbol{\rho}_1) = 1\}\}.$$

Taking into account expressions (2) and (2a) and the fact that

$$P\{\xi_m(\boldsymbol{\rho}) = 1 / \xi_n(\boldsymbol{\rho}) = 1\} + P\{\xi_m(\boldsymbol{\rho}) = 0 / \xi_n(\boldsymbol{\rho}) = 1\} = 1,$$

$$P\{\xi_m(\boldsymbol{\rho}_2) = 1 / \xi_m(\boldsymbol{\rho}_1) = 0\} = p_m\, [1 - \exp\{- A(\boldsymbol{\omega}) \times |\boldsymbol{\rho}_1 - \boldsymbol{\rho}_2|\}],$$

we obtain relation (5).

The mathematical expectation and variances of the fields $\xi_m(\boldsymbol{\rho})$, $m = 1, 2, \ldots, M$, equal, respectively,

$$M\xi_m(\boldsymbol{\rho}) = p_m, \quad D\xi_m(\boldsymbol{\rho}) = p_m\,(1 - p_m).$$

The normalized correlation functions $B_{nm}(\boldsymbol{\rho}_1, \boldsymbol{\rho}_2)$ between indicators of different layers $\{\xi_m(\boldsymbol{\rho})\}$, $m = 1, 2, \ldots, M$, have the form

$$B_{nm}(\boldsymbol{\rho}_1, \boldsymbol{\rho}_2) = \frac{K_{nm}(\boldsymbol{\rho}_1, \boldsymbol{\rho}_2)}{\sqrt{D\xi_n(\boldsymbol{\rho})\, D\xi_m(\boldsymbol{\rho})}} = \frac{P_{nm} - p_n\, p_m}{\sqrt{p_n\,(1 - p_n)\, p_m\,(1 - p_m)}} \times \exp\{- A(\boldsymbol{\omega}) \times |\boldsymbol{\rho}_1 - \boldsymbol{\rho}_2|\}. \quad (6)$$

The correlation coefficients $b_{nm} = B_{nm}(\boldsymbol{\rho}_1, \boldsymbol{\rho}_2)$ satisfy the relation

$$b_{nm} \in \left[-\sqrt{\frac{p_n p_m}{(1 - p_n)(1 - p_m)}},\ \frac{\min(p_n, p_m) - p_n p_m}{\sqrt{p_n (1 - p_n) p_m (1 - p_m)}} \right]. \quad (7)$$

The least possible value $b_{nm} = -1$ is reached only when $p_n + p_m = 1$ (so that $Q_{nm} = Q_{mn} = 0$, $\bar{Q}_{nm} = \bar{Q}_{mn} = 1$); while the maximum value $b_{nm} = 1$ is reached when $p_n = p_m$ (so that $Q_{nm} = Q_{mn} = 1$, $\bar{Q}_{nm} = \bar{Q}_{mn} = 0$).

Overall, the Poisson model of M-layer broken clouds is defined by the parameters A_x and A_y (intensities of point fluxes along OX and OY axes, respectively), as well as by the probabilities

$$P(\xi_m(\boldsymbol{\rho}) = a_m,\ m = 1, 2, \ldots, M),$$

where $a_m = 0$ or $a_m = 1$, for 2^M possible combinations of $(a_1, a_2, \ldots, a_M)$. Since

$$\sum_{(a_1, a_2, \ldots, a_M)} P(\xi_m(\boldsymbol{\rho}) = a_m,\ m = 1, 2, \ldots, M) = 1,$$

a total of $(2^M - 1)$ probabilities must be specified in order to describe the Poisson model of the M-layer clouds.

The cloud fraction of the mth layer N_m coincides with the probability of cloud occurrence: $N_m = p_m$. The total cloud amount p of M-layer clouds is defined as

$$p = 1 - P\{\xi_1(\boldsymbol{\rho}) = 0,\ \xi_2(\boldsymbol{\rho}) = 0,\ \ldots,\ \xi_M(\boldsymbol{\rho}) = 0\}, \quad (8)$$

while the range of p variations is given by

$$\max(p_1, p_2, \ldots, p_M) = p_{\max} \le p \le p_{\min} = \min\left(\sum_{i=1}^{M} p_i,\ 1 \right). \quad (9)$$

The quantities $p_{\min}$ and $p_{\max}$ correspond to the total cloud amount of M-layer clouds for hypotheses of “minimum” and “maximum” overlap.

1.3. Two-layer model of broken clouds

Let us consider a two-layer cloud model in a more detail. In this section, the subscript “1” will refer to the lower layer, and subscript “2” to the upper layer. Instead of the probabilities

$$P(\xi_m(\boldsymbol{\rho}) = a_m,\ m = 1, 2),$$

where a_m is either 0 or 1, we can use as a model parameter, the cloud fraction p_j of one of the cloud layers, and the conditional probabilities

$$Q_{ij} = P\{\xi_i(\boldsymbol{\rho}) = 1 / \xi_j(\boldsymbol{\rho}) = 1\},$$

$$\bar{Q}_{ij} = P\{\xi_i(\boldsymbol{\rho}) = 1 / \xi_j(\boldsymbol{\rho}) = 0\}, \quad i \ne j.$$

The cloud fractions for different layers are related as (see Ref. 4):

$$p_1 = Q_{12}\, p_2 + \bar{Q}_{12}\,(1 - p_2), \qquad p_2 = Q_{21}\, p_1 + \bar{Q}_{21}\,(1 - p_1). \quad (10)$$

According to relation (8), for total cloud amount p, a number of simple relations can be obtained

$$p = P\{\xi_1(\boldsymbol{\rho}) = 1, \xi_2(\boldsymbol{\rho}) = 1\} + P\{\xi_1(\boldsymbol{\rho}) = 1, \xi_2(\boldsymbol{\rho}) = 0\} + P\{\xi_1(\boldsymbol{\rho}) = 0, \xi_2(\boldsymbol{\rho}) = 1\} = p_1\, Q_{21} + p_1\,(1 - Q_{21}) + p_2\,(1 - Q_{12}) = p_1 + p_2 - p_2\, Q_{12} = p_1 + p_2 - p_1\, Q_{21} = p_1 + p_2 - P_{12}. \quad (11)$$

Thus, for instance, if the quantities p_1, Q_{21}, and $\bar{Q}_{21}$ are known, then p_2 [see Eq. (10)] and p can be uniquely determined:

$$p = p_1 + \bar{Q}_{21}\,(1 - p_1). \qquad (12)$$

From Eq. (10) it follows that, for a fixed p_1, the cloud fraction p_2 depends both on Q_{21} and $\bar{Q}_{21}$ (Fig. 1); whereas the total cloud amount p is determined only by $\bar{Q}_{21}$ [see Eq. (12)].

If $Q_{21} = 1$ and $\bar{Q}_{21} = 0$, then $p = p_1 = p_2$, while the correlation coefficient $b_{12} = 1$: thus, this cloud realization corresponds to the case when the *cloud in one layer over- (under-) lies the cloud in the other layer*. If $Q_{21} = 0$ and $\bar{Q}_{21} = 1$, then $p_2 = 1 - p_1$, $p = 1$, and $b_{12} = -1$: thus, in this case the clouds in one layer overly cloud gaps in the other layer ("checkerboard pattern"). Figure 2 presents the realizations of cloud field for intermediate values of conditional probabilities Q_{21} and $\bar{Q}_{21}$.

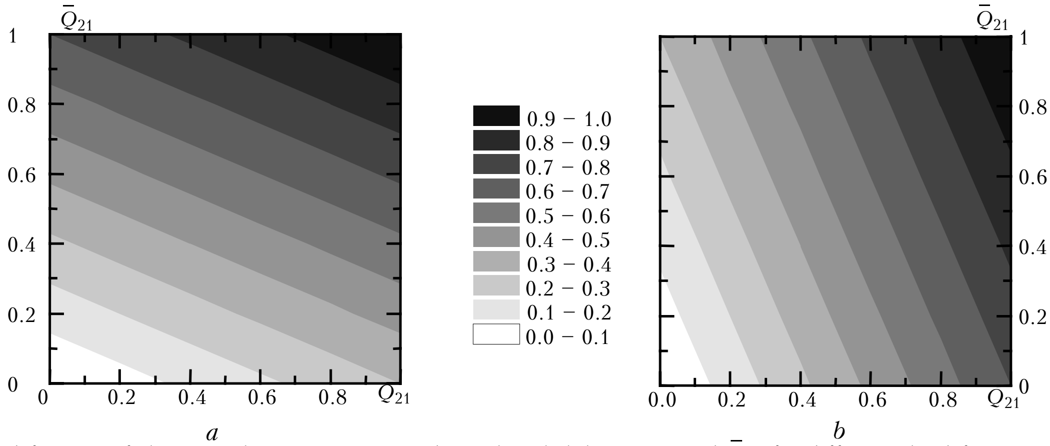

Fig. 1. Cloud fraction of the upper layer p_2 versus conditional probabilities Q_{21} and $\bar{Q}_{21}$ for different cloud fractions of the lower layer: (*a*) $p_1 = 0.3$ and (*b*) $p_1 = 0.7$.

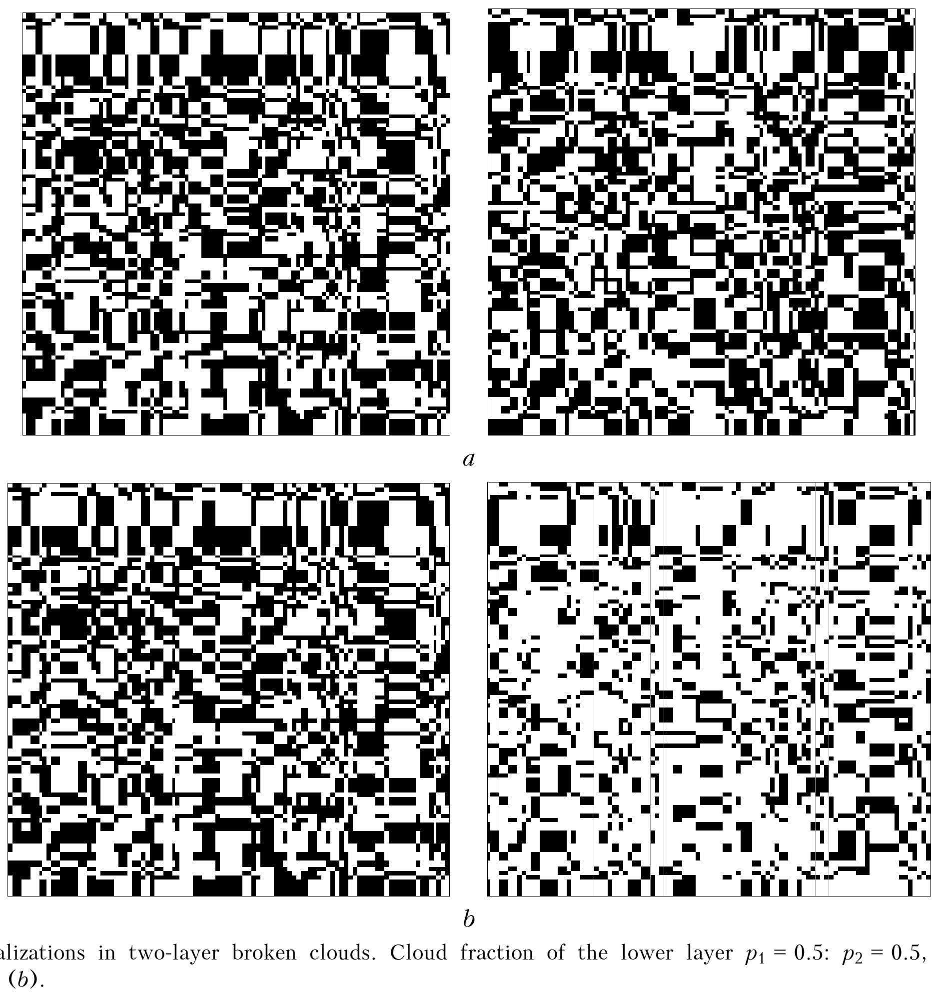

Fig. 2. Cloud realizations in two-layer broken clouds. Cloud fraction of the lower layer $p_1 = 0.5$: $p_2 = 0.5$, $p = 0.75$ (*a*) and $p_2 = 0.7$, $p = 0.85$ (*b*).

Note that a sufficient set of parameters of two-layer model ($M = 2$) may include total cloud amount p and cloud fractions p_j ($j = 1, 2$) of each of the layers (this information is sufficient for describing the model with the number of layers M in excess of two).

2. Mean solar radiative fluxes for two-layer cloud model

In this section we present results of numerical experiment using Monte Carlo method to estimate the influence of variations of parameters $\bar{Q}_{21}$ and Q_{21} on the mean albedo R (at the top of the atmosphere) and diffuse transmittance Q_s (at the surface level). In analysis of the results we will keep in mind that the increase (decrease) of Q_{21} for a fixed $\bar{Q}_{21}$ is equivalent to increase (decrease) of cloud fraction in the upper cloud layer p_2 for a fixed total cloud amount p [Eq. (11) and (12)]. The variations of $\bar{Q}_{21}$ for a given Q_{21} suggest a simultaneous variation of both p_2 and p.

The mean fluxes of solar radiation at different atmospheric levels are calculated for the model described, e.g., in Ref. 21. It was assumed that a unit flux of solar radiation is incident on the top of the atmosphere along the direction $\boldsymbol{\omega}_\upsilon = (\xi_\upsilon, \varphi_\upsilon)$, where ξ_υ and φ_υ are the solar zenith and azimuth angles. The calculations are made for the following parameters: the lower cloud layer is located at the height of 3 to 3.25 km, and the upper level is at height 3.5 – 3.75 km; the extinction coefficient in the cloud layers σ is 20 km^{-1}, absorption in the clouds was not considered; the intensities of Poisson fluxes A_x and A_y were calculated from formula (3) assuming that the mean horizontal sizes of the cloud elements $D_x = D_y = 0.25$ km for the lower layer. The cloud field was simulated in a 3×3 km^2 domain assuming periodic boundary conditions. The scattering phase function for C_1 cloud (wavelength $\lambda = 0.69$ μm) from Ref. 22 was used as the cloud scattering phase function. We present the calculated results for the surface albedo $A_s = 0.0$.

Figure 3 presents the mean values of albedo R and diffuse transmittance Q_s as functions of conditional probabilities $0 \le Q_{21} \le 1$ and $0 \le \bar{Q}_{21} \le 1$. If the parameter $\bar{Q}_{21}$ is fixed (i.e., the total cloud amount p is preset), with the increase in Q_{21} the mean albedo may increase by as much as approximately 0.1–0.15.

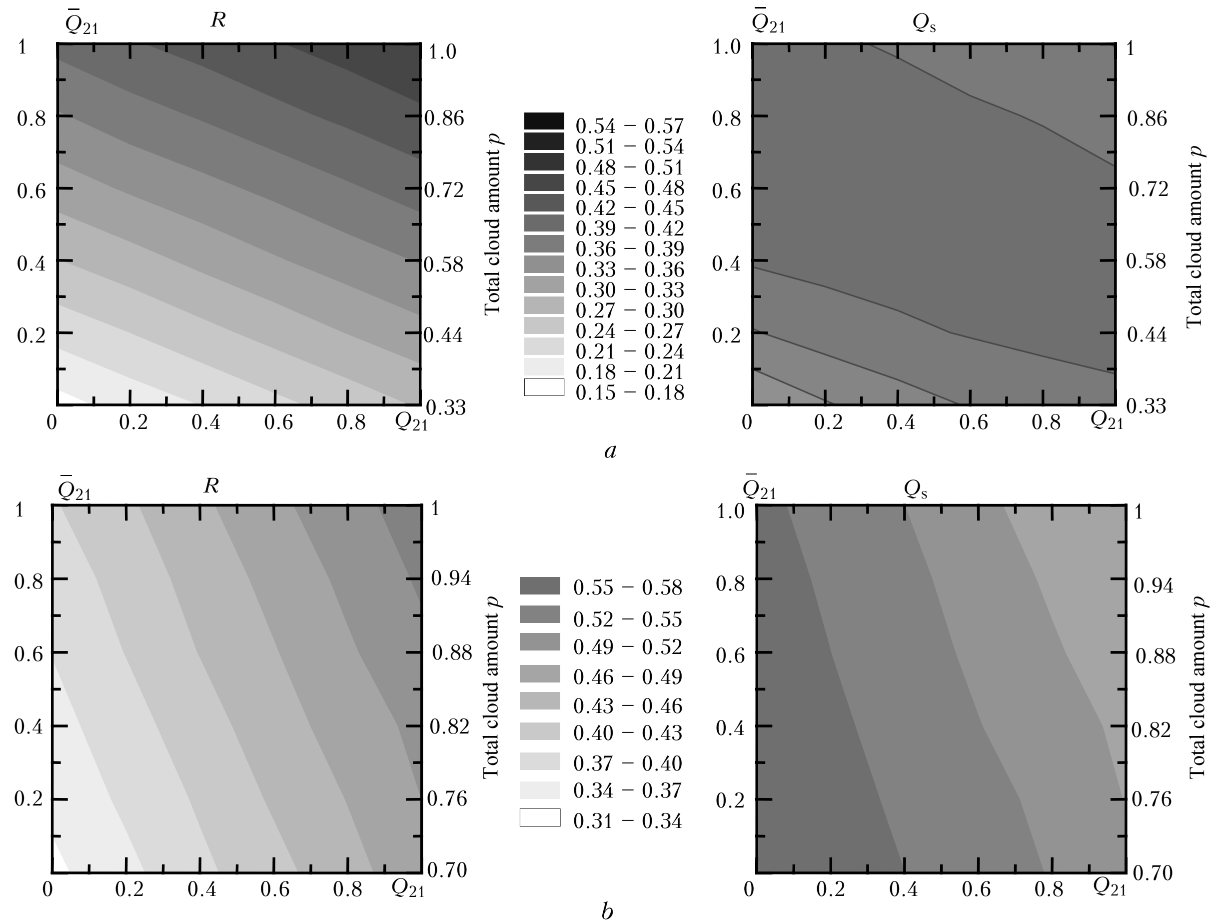

Fig. 3. Mean values of albedo R and diffuse transmittance Q_s versus $0 \le Q_{21} \le 1$ and $0 \le \bar{Q}_{21} \le 1$ for a fixed cloud fraction of the lower layer $p_1 = 0.3$ (*a*); and 0.7 (*b*). Solar zenith angle $\xi_\upsilon = 60°$, cloud extinction coefficient $\sigma = 20$ km^{-1}, mean cloud sizes in the lower layer $D_x = D_y = 0.25$ km, and the mean surface albedo $A_s = 0.0$.

For a given Q_{21} and increasing $\bar{Q}_{21}$, the total cloud amount p increases from $p = p_1$ to $p = 1$. Therefore, the greater the cloud fraction of the lower layer p_1, the less the range of p variations, and, hence, the weaker the variations of the mean albedo with the increasing $\bar{Q}_{21}$. The aforesaid is supported by calculated results on albedo, presented in Fig. 3: the albedo increases by ≈ 0.2 for $p_1 = 0.3$ and by ≈ 0.05–0.07 for $p_1 = 0.7$.

As known, in single-layer clouds, the diffuse transmittance, as a function of cloud optical depth and/or cloud fraction, reaches a maximum whose position and magnitude depend on solar zenith angle. A similar Q_s property is also observed for multilayer clouds: for instance, the mean diffuse transmittance depends nonmonotonically on $\bar{Q}_{21}$ (and hence on p) for $p_1 = 0.3$ and for a fixed $Q_{21} \geq 0.3$ (Fig. 3*a*). At small and intermediate cloud fractions $p \leq 0.5$–0.6 (of course, assuming that the cloud fraction in the lower layer p_1 is also small), an increase in Q_{21} leads to a growth of Q_s; whereas at $p > 0.6$, the reverse is true.

Let us discuss how the mean radiative fluxes, calculated using the cloud model described above, compare with those, calculated by the Poisson model of broken clouds,[14] in which the cloud layers are assumed statistically independent (the characteristics in the model of statistically independent layers[14] will be denoted by the superscript ind). If the total cloud amount p and cloud fraction of the lower layer p_1 are kept constant, in the model with statistically independent cloud fields the available information on p and p_1 uniquely determines the cloud fraction of the upper layer:

$$p_2^{\text{ind}} = (p - p_1)/(1 - p_1).$$

Within the approach proposed here, for the same p and p_1, there may be a family of models, each having its own cloud fraction in the upper layer.

We will compare the mean radiative fluxes calculated for the same p and p_1 (and the horizontal cloud sizes selected accordingly for both models). If Q_{21} varies in the entire range of possible values and, hence, the cloud fraction of the upper layer varies in the range $0 \leq p_2 \leq 1$, then the difference of the mean fluxes $\Delta F = F - F^{\text{ind}}$, $F = R, S, Q_s$, may reach ≈ 0.1–0.2 (Fig. 4). However, if assuming

$$Q_{21} = \bar{Q}_{21} = (p - p_1)/(1 - p_1),$$

one obtains a model with correlated cloud layers in which

$$p_2 = (p - p_1)/(1 - p_1).$$

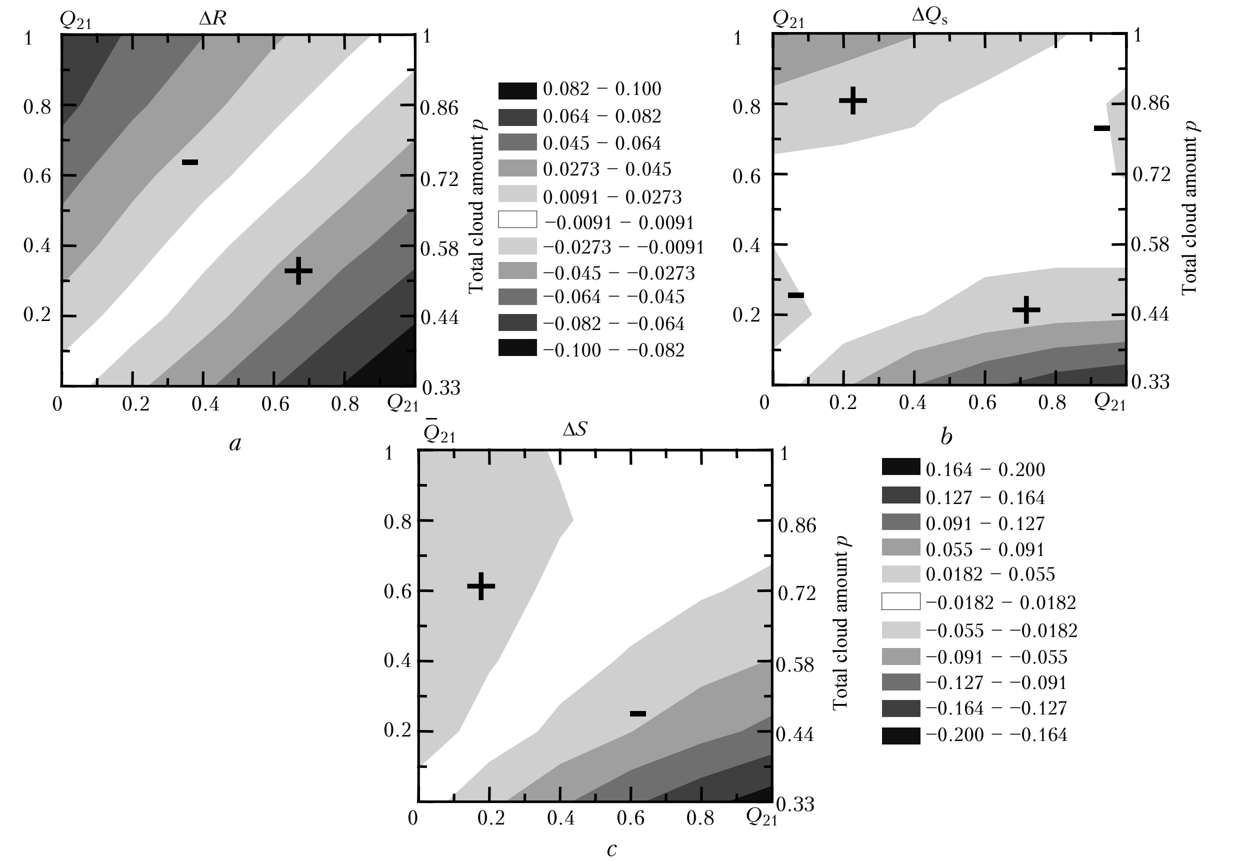

Fig. 4. Difference between mean albedos (*a*), diffuse transmittances (*b*), and nonscattered fluxes (*c*), calculated in the cloud model suggested here and in the model by Titov[14]: $\Delta F = F - F^{\text{ind}}$, $F = R, Q_s, S$. The calculations are made for $p_1 = 0.3$; the other parameters being the same as in Fig. 3.

Thus we have discussed two models, the model by Titov[14] and the model proposed in this paper; these have the same p, p_1, and $p_2 = p_2^{\text{ind}}$, and differ in that in the latter model the cloud realizations within the upper and lower layers are constructed on the same Poisson point fluxes. The calculated results show that, when $p_2 = p_2^{\text{ind}}$, the differences between transmitted (both diffuse Q_s and nonscattered S) and reflected fluxes, calculated in the two models considered here, are within 0.01–0.02. This suggests that, at $p_2 = p_2^{\text{ind}}$, the mean radiative fluxes little depend on how the cloud realizations in the upper layer are constructed.

Conclusion

The model of multilayer broken clouds proposed, based on the Poisson point fluxes, has the following features:

– the input model parameters have clear physical meaning and may be quite easily determined from the experimental data; and

– the model allows for a wide range of correlations between different cloud layers, constituting a natural generalization of the known single-layer Poisson model.

This model can be used to study the processes of radiative transfer in multilayer clouds, caused by the presence of correlations between clouds at different atmospheric levels. In particular, our calculations using the model of two-layer clouds have shown that, for fixed cloud fractions of the lower layer and total cloud amount (it is exactly the two characteristics that are followed up at meteorological stations) correlations between the cloud layers can substantially affect the radiative characteristics of a cloud system.

Now we would like to conclude by noting that the absence of sufficient information on probabilistic characteristics of the spatial structure of cloud fields is the common problem in model development and testing. However, the fact that recently the integrated studies of complex cloud systems have been receiving more and more attention (see, e.g., Refs. 23–25) proves the grounds to believe that such information will be obtained and, as a consequence, more adequate stochastic cloud models will be developed in the nearest future.

Acknowledgment

The work is performed as part of scientific research project under support of the Russian Foundation for Basic Research (Grants 00–05–65456, 00–01–00797, and 00–15–96173), INTAS–01–0239, and SB RAS (Integration Grant 2000, No. 43).

References

1. I.P. Mazin and A.Kh. Khrgian eds., *Clouds and the Cloudy Atmosphere* (Gidrometeoizdat, Leningrad, 1989), 647 pp.
2. S. Manabe and R.F. Strickler, J. Atmos. Sci. **21**, 361–385 (1964).
3. J.F. Geleyn and A. Hollingsworth, Contrib. Atmos. Phys. **52**, 1–16 (1979).
4. L. Tian and J.A. Curry, J. Geophys. Res. D **94**, 9925–9935 (1989).
5. X.-Z. Liang and W.-C. Wang, J. Geophys. Res. D **102**, No. 10, 11039–11047 (1997).
6. C.J. Stubenrauch, A.D. Del Genio, W.B. Rossow, J. Climate, No. 2, 273–287 (1997).
7. V.E. Zuev and G.A. Titov, *Atmospheric Optics and Climate* (Spektr Publishing House of IAO SB RAS, Tomsk, 1996), 271 pp.
8. R.F. Cahalan, W. Ridgway, W.J. Wiscombe, T.L. Bell, and J.B. Snider, J. Atmos. Sci. **51**, No. 16, 2434–2455 (1994).
9. A. Marshak, A. Davis, R.F. Cahalan, and W.J. Wiscombe, Phys. Rev. E **49**, 55–79 (1994).
10. S.M. Prigarin and G.A. Titov, Atmos. Oceanic Opt. **9**, No. 7, 629–635 (1996).
11. S.M. Prigarin, B.A. Kargin, and U.G. Oppel, Pure and Appl. Opt. A **7**, No. 6, 1389–1402 (1998).
12. S.M. Prigarin, N.I. Gubina, and U.G. Oppel, in: *IRS 2000: Current Problems in Atmospheric Radiation* (A. Deepak Publishing, Hampton, Virginia, 2001), pp. 257–260.
13. L. Oreopoulos and H. Barker, Quant. J. Roy. Meteorol. Soc., No. 125, 301–333 (1999).
14. G.A. Titov and T.B. Zhuravleva, Atmos. Oceanic Opt. **12**, No. 3, 196–203 (1999).
15. G.A. Titov and E.I. Kassianov, Atmos. Oceanic Opt. **12**, No. 10, 873–882 (1999).
16. G.N. Glazov and G.A. Titov, Izv. Vyssh. Uchebn. Zaved., Ser. Fizika **23**, No. 4, 424–431 (1980).
17. V.N. Skorinov and G.A. Titov, Izv. Vyssh. Uchebn. Zaved., Ser. Radiofizika **26**, No. 8, 971–980 (1983).
18. G.A. Titov, Izv. Akad. Nauk SSSR, Ser. Fiz. Atmos. Okeana **21**, No. 9, 940–948 (1985).
19. G.A. Titov, Izv. Vyssh. Uchebn. Zaved., Ser. Radiofizika **26**, No. 8, 966–970 (1983).
20. T.B. Zhuravleva and G.A. Titov, in: *Optical and Meteorological Studies of the Earth Atmosphere*, G.M. Krekov and V.S. Komarov, eds. (Nauka, Novosibirsk, 1987), pp. 108–119.
21. G.A. Titov and T.B. Zhuravleva, Atmos. Oceanic Opt. **10**, No. 7, 437–446 (1997).
22. D. Deirmendjian, *Electromagnetic Waves Scattering on Spherical Polydispersions* (American Elsevier, New York, 1969), 290 pp.
23. J. Wang and W.A. Rossow, J. Appl. Meteorol. **34**, No. 10, 2243–2258 (1995).
24. J. Bergman and H.H. Hendon, J. Atmos. Sci. **55**, 3471–3491 (1998).
25. J. Wang, W.A. Rossow, T. Uttal, and M. Rozendaal, Mon. Weath. Rev. **127**, 2484–2502 (1999).